Available at www.sciencedirect.com

ScienceDirect

journal homepage: www.elsevier.com/locate/he

Characteristics of plasma induced by interaction of a free-oscillated laser pulse with a coal target in air and combustible gas

Qiansuo Yang, Zhimin Peng*

Laboratory of High Temperature Gas Dynamics, Institute of Mechanics, Chinese Academy of Sciences, Bei-si-huan-xi-lu No.15, Beijing 100190, China

ARTICLE INFO

Article history:
Received 27 October 2009
Received in revised form
9 December 2009
Accepted 9 December 2009
Available online 25 March 2010

Keywords:
Plasma
Free-oscillated Nd:YAG laser
Laser ignition
Radical spectrum
Hydrogen-oxygen mixture

ABSTRACT

Plasma in the air is successfully induced by a free-oscillated Nd:YAG laser pulse with a peak power of 10^{2-3} W. The initial free electrons for the cascade breakdown process are from the ablated particles from the surface of a heated coal target, likewise induced by the focused laser beam. The laser field compensates the energy loss of the plasma when the corresponding temperature and the images are investigated by fitting the experimental spectra of $B^2\sum^+ \rightarrow X^2\sum^+$ band of CN radicals in the plasma with the simulated spectra and a 4-frame CCD camera. The electron density is estimated using a simplified Kramer formula. As this interaction occurs in a gas mixture of hydrogen and oxygen, the formation and development of the plasma are weakened or restrained due to the chaining branch reaction in which the OH radicals are accumulated and the laser energy is consumed. Moreover, this laser ignition will initiate the combustion or explosion process of combustible gas and the minimum ignition energy is measured at different initial pressures. The differences in the experimental results compared to those induced by a nanosecond Q-switched laser pulse with a peak power of 10^{6-8} W are also discussed.

1. Introduction

The induction of plasma in air or other gases by a laser pulse is usually via inverse *Bremsstrahlung* process, and the initial free electrons for this cascade process are essential [1]. As a laser pulse with a wavelength of ≥250 nm is employed to induce the plasma in the gas, a gaseous molecule or atom has to simultaneously absorb a number of photons for these free electrons since the photon energy is usually lower than the ionization potential [1–5]. Therefore, multi-photon ionization process is the only origin of initial free electrons in clean gas without external preionization [1]. Consequently, a strong electromagnetic field is usually required for the breakdown of the gas primarily through the multi-photon ionization process. On the other hand, Stark shifting, the overlapping of the upper energy levels into a quasi-continuum energy band, and the broadening of the intermediate energy levels under a strong laser field are all beneficial for enhancing ionization [6]. However, not only does the production of such a laser pulse for the multi-photon ionization process require the insertion of a Q-switcher in the resonant cavity [7–11], this type of laser beam cannot be delivered in a flexible optical fiber system because the corresponding peak power is higher than the damage threshold of multi-mode silicon fiber [6]. Therefore, plasma or sparks induced by such a laser pulse are expensive and inflexible in practical application, such as for laser ignition initiation of certain combustion processes.

In the process of a laser-induced plasma or spark in a gas, only the production of the initial free electrons through the multi-photon ionization requires a strong laser field. If these

* *Corresponding author.*
E-mail address: qsyang@imech.ac.cn (Q. Yang).
0360-3199/$ – see front matter
doi:10.1016/j.ijhydene.2009.12.045

electrons can be provided via other methods, the electron cascade process is carried out under a laser beam with a weaker light field than that used for multi-photon ionization. The previous experiments have revealed that the preionization and impurity in the gas result in the decrease of the breakdown energy threshold [12,13]. To our knowledge, however, no study has yet been done on plasma in gas induced by free-oscillated Nd:YAG laser with a low peak power. This type of laser device not only produces a pulse profile with a duration of 10^{2-3} μs, which contains a number of oscillated pulses with a peak power of 10^{2-3} W that is much weaker than a nanosecond Q-switched laser pulse with a peak power of 10^{6-8} W, it is not as attractive as Q-switched laser. The production of a weak and long laser pulse is due to the lack of a Q-switch device in the resonant cavity. However, this type of laser beam can be propagated in the fiber optical core since the peak power is much lower than the damage threshold of the multi-mode optical fiber with a diameter of 0.5 mm [6].

In this paper, experiments conducted on the induction of plasma in air by a free-oscillated Nd:YAG laser pulse, as well as initial free electrons produced through the interaction of the laser pulse with a coal target are reported and analyzed. The temperature of the plasma is measured by the rotation and vibration temperatures of CN radials, which are determined by the spectral structure of the $B^2\Sigma^+ \rightarrow X^2\Sigma^+$ band [14,15]. A 4-frame CCD camera is employed to analyze the evolution of plasma in air and combustible gas. The lifetimes of the plasma are approximately equal to the pulse duration of the laser because the energy loss of the plasma is compensated by the laser pulse. The corresponding electron density is estimated according to a simplified Kramer formula [7]. On the other hand, as the interaction above occurs in a combustible gas (mixture of hydrogen and oxygen), the formation and development of plasma are weakened or restrained due to the chaining branch reaction that produce OH radicals. Moreover, a combustion or explosion of the mixed gas, which depends on the initial pressure, is initiated by this interaction and the minimum ignition energy decreases with the increasing of the initial pressure. The differences of the experimental results from those induced by a nanosecond Q-switched laser pulse with a peak power of 10^{6-8} W are discussed.

2. Experimental setup

The experimental setup for the interaction of free-oscillated laser pulse with a coal target is shown in Fig. 1. The laser pulse is produced by a free-oscillated Nd:YAG laser with a wavelength of 1064 nm. The duration and the energy of a pulse are 200 μs and up to 800 mJ, respectively. The volume of the combustion cell is 160 × 160 × 100 mm^3. Four blocks of silicon window with an area of 85 × 48 mm^2 are mounted on the sides of the cell for the incidence of the laser pulse, the recording of the experimental spectrum, and the capturing of the images. At a height of 55 mm and a distance of 105 mm from the incidence window, a coal target with a plane is fixed toward the laser pulse, as shown in Fig. 1. A lens with a focal length of 150 mm is employed to focus the laser beam onto the coal target. The distance between the lens and the target is approximately equal to the focal length within an error of 10 mm. The cell can then be filled with air or the gas mixture.

On the left side of the cell, a four-frame CCD camera with an exposure time of 20 μs is utilized to capture the succession of plasma images, and an optical multi-channel analyzer (OMA) is set on the right side for the spectrum of the $B^2\Sigma^+–X^2\Sigma^+$ band of CN radicals and the $A^2\Sigma^+–X^2\Pi$ band of OH radicals in order to determine the rotation and vibration temperatures of CN radicals and the existence of OH radicals. In the experiment, the appearance of the laser pulse is the trigger signal for the four-frame CCD camera and OMA. The delay time ΔT of each frame and OMA can be adjusted. A mercury lamp is used to measure the optical apparatus function of the OMA for the fitting of the experimental spectrum with the simulated one.

3. In air experimental results and discussion

For the air at atmospheric condition, by fitting the experimental spectrum of the $B^2\Sigma^+ \rightarrow X^2\Sigma^+$ band of CN radicals with the simulated spectrum, the rotation temperature and vibration temperature of the corresponding simulated spectrum is determined, as shown in Fig. 2(a) and (b). The

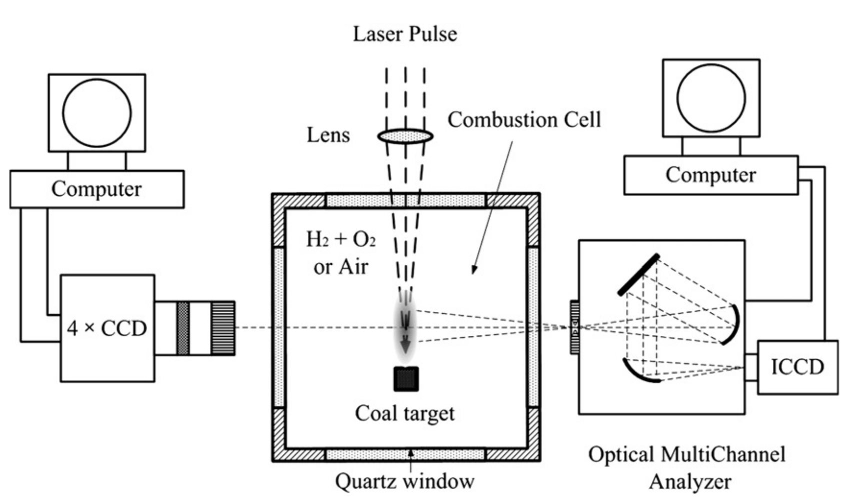

Fig. 1 – Experimental setup.

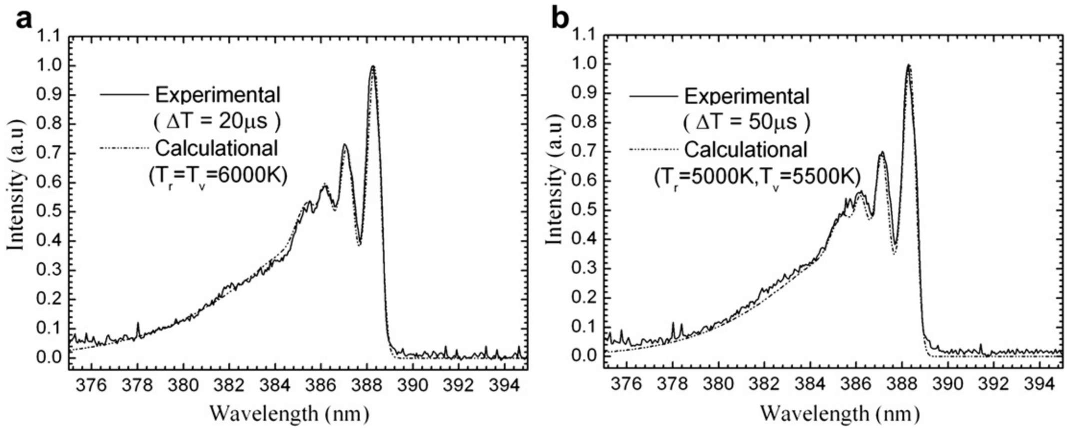

Fig. 2 – Experimental and simulated spectrum of $B^2\sum^+ \rightarrow X^2\sum^+$ band of CN radicals for the rotation and vibration temperatures at (a) $\Delta T = 20\ \mu s$ and (b) $\Delta T = 50\ \mu s$.

experimental results display that the two temperatures are initially equal to each other, but rotation temperature decreases faster than vibration temperature. For a 100 mJ laser, the initial temperatures are initially about 6000 K, and rises along with the increase of laser energy. As the energy of a laser pulse increases to 500 mJ, the temperatures reach as high as 9000 K. Therefore, the temperature of the plasma is proportional to the level of laser energy. The detailed process for the determination of two temperatures will be described in another paper. Because CN radicals are contained in the plasma, it is reasonable to assume that the temperatures of CN radicals are considered to be equal to the temperature of the plasma under equilibrium states.

Fig. 3 shows the images of the plasma induced by a laser pulse of 100 mJ. The area of the images are $18 \times 24\ mm^2$, with different delay times for four occasions of plasma formation.

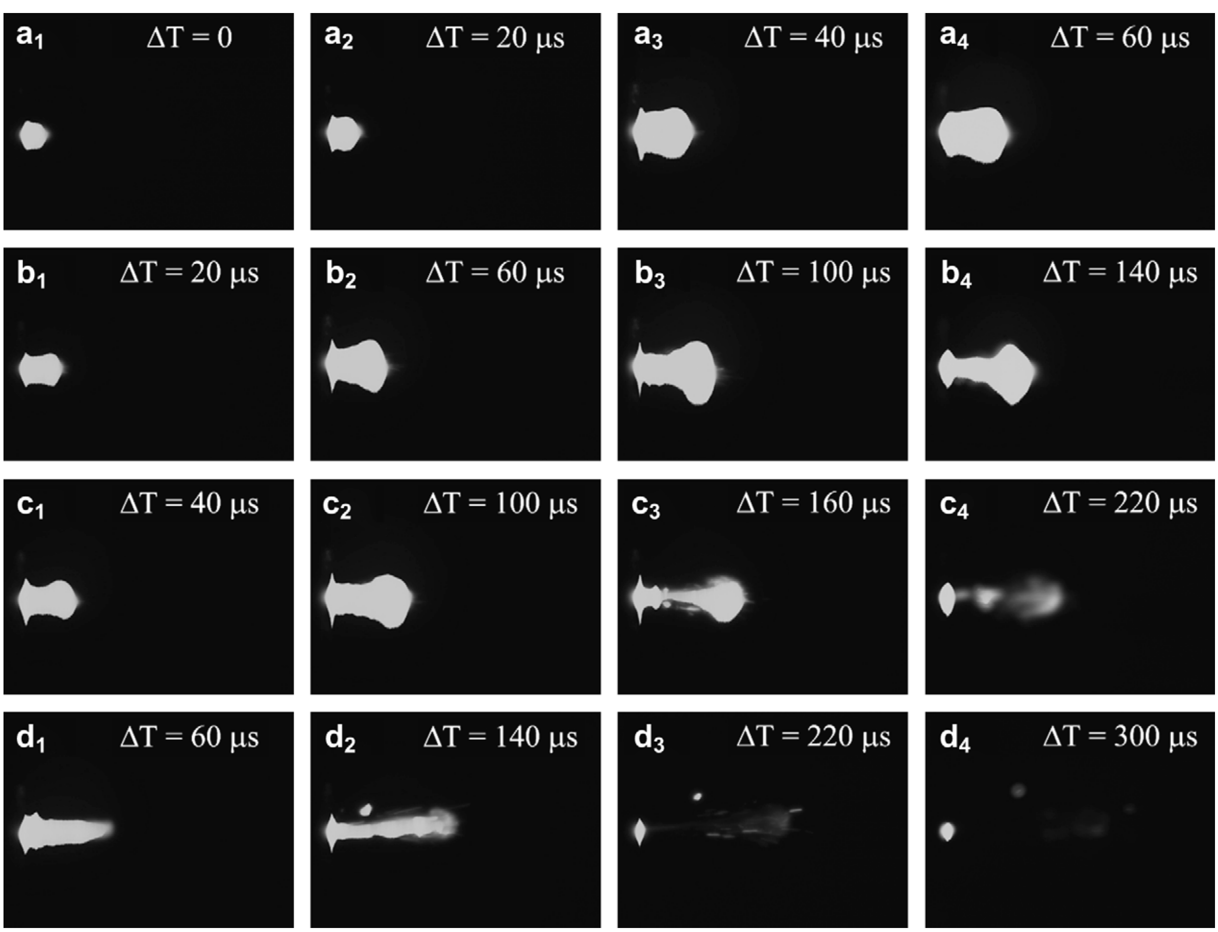

Fig. 3 – Images of plasma in the air with a pressure of 60 kPa as the energy of each laser pulse is about 100 mJ.

The production of the trigger signal is simultaneous with the laser pulse onset. Fig. 3 also shows that the spatial region of the plasma gradually increases during the duration of the laser pulse. However, after the laser pulse passes, the radiation of the plasma begins to decrease, as shown in Fig. 3 (c_4) and (d_3), because the light pulse lasts about 200 μs. It can therefore be concluded that the lifetime of the plasma is approximately equal to the pulse width of the laser beam. This is consistent with the previous experiment investigating the plasma ionization level [16]. The characteristics above are based on the energy loss of the plasma, which results from the diffusion of the electron outside the plasma and the radiation of the plasma [4–6], being compensated by the laser energy.

Fig. 4 shows the images of the plasma under five pressures: 80 kPa, 40 kPa, 20 kPa, 10 kPa, and ≤50 Pa, where the energy of each laser and the area of the images are the same as those in Fig. 3. Compared to the previous experiment [8,9], the scales of the plasma in Fig. 4(a)–(d) are all larger by one order of magnitude than those induced by a nanosecond Q-switched laser pulse. By considering this, and the fact that its temperature is much lower than that induced by a Q-switched pulse [8,9], it is apparent that the energy loss due to the radiation is more serious for the plasma induced via Q-switched laser pulse. There are two possible reasons for result: First, a photon due to the transitioning from the upper to the lower level has a high probability of being resonantly absorbed by an atom, molecule, or ion in the plasma with a long path. Second, the radiation intensity of the plasma is proportional to its temperature [4–6].

For the deposition of laser energy in the plasma, the production of the plasma through the interaction of a free-oscillated laser pulse with a target is more efficient than the gas breakdown by a Q-switched laser pulse. As the duration of a Q-switched pulse is on the order of 10^{-8} s, the sudden

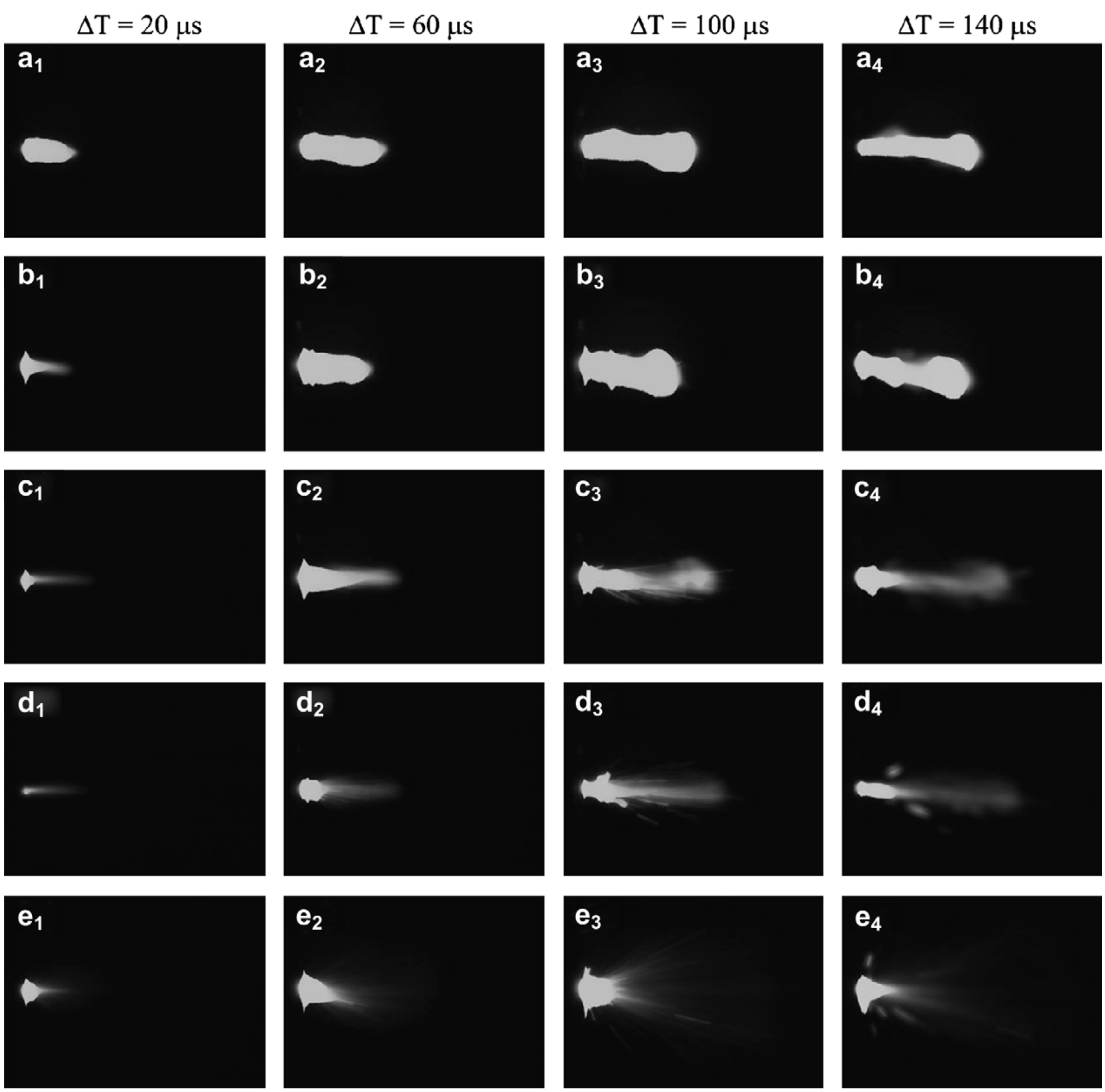

Fig. 4 – Images of plasma in the air with pressures of ($a_{1–4}$) 80 kPa, ($b_{1–4}$) 40 kPa, ($c_{1–4}$) 20 kPa, ($d_{1–4}$) 10 kPa, and ($e_{1–4}$) ≤50 Pa.

appearance and the rapid expansion due to the production of a strong blast wave or shock wave due to high temperature and tremendous pressure, results in the substantial loss of the laser energy in the blast wave [6]. On the other hand, for the free-oscillated laser pulses, as shown in Fig. 4(a)–(d), the expansion of the plasma is slower than the sound speed; therefore, the loss of the energy in the expansion wave is with a small percentage loss for a laser pulse. Thus, the deposition of laser energy into the plasma through the interaction of a free-oscillated laser pulse with a target is more effective than the cascade breakdown induced by a Q-switched laser pulse; it is therefore more appropriate for the practical application of laser ignition.

As the interaction above occurs in the air with a pressure lower than 50 Pa, the small-size plasma only forms in the front of the target, as shown in Fig. 4(e_{1-4}). This phenomenon points out that most of the ionized molecules are gas molecules. At the beginning of the cascade process, the ionized molecules may be the particles ablated from the target. However, as the plasma gradually forms, these particles rapidly escape from the focal volume [16]. The molecules for the cascade breakdown process only come from the gas around the plasma; however, as air density is so low that the air around the plasma cannot provide enough molecules for the cascade breakdown process, the development of the plasma is weakened or suppressed. In Fig. 4(e_{1-4}), the rays around the plasma correspond to the diffusion of free electrons outside the plasma, showing that the free path increases as the pressure decreases.

Electron density can be estimated by substituting the above values of the temperature and the length of the plasma into the Kramer formula. From the images in Figs. 3 and 4, the part of the plasma near the target lasts as long the duration of the pulse. Since we assume its energy losses are also compensated by the laser beam, it is reasonable to also assume that the effective absorption distance is defined as the length of the plasma. The simplified Kramer formula is as follows [7]:

$$k_e = 3.69 \times 10^8 \frac{n_e^2}{\nu^3 \sqrt{T}} \left[1 - \exp\left(-\frac{h\nu}{kT}\right)\right] \quad (1)$$

where k_e and T are the effective absorption coefficient and the temperature of the plasma, respectively, ν is the laser frequency, n_e is the electron density, h and k are Plank's and Boltzmann's constants, respectively. For $\nu = 2.8195 \times 10^{14}$ Hz, $h = 6.625 \times 10^{-27}$ erg s, $k = 1.38 \times 10^{-16}$ erg/K, $k_e = 1$ cm^{-1}, $T = 6400$ K, the corresponding electron density n_e is obtained: $n_e = 2.066 \times 10^{18}$ cm^{-3}, which is lower by one order of magnitude than the molecule density ($n_0 = 2.69 \times 10^{19}$ cm^{-3}) of the air at the atmospheric condition and is also lower than the electron density of the plasma induced by a Q-switched laser pulse [8].

4. In combustible gas experimental results and discussion

As the interaction of free-oscillated laser pulse with the target occurs in a combustible mix of hydrogen and oxygen, the formation and development of plasma are also weakened or restrained because the laser energy, through an unknown process, is consumed by the chaining branch reaction, in which the OH radicals are accumulated. Furthermore, the production of OH radicals will initiate the combustion or the explosion of the combustible gas, depending on the initial pressure of the gas. For the premixed hydrogen and oxygen (H_2:O_2 = 2:1), the pressure threshold for the explosion is in the range of 86–90 kPa at room temperature.

Fig. 5(a) and (b) shows the images around the focal point at two moments as the initial pressure of the premixed gas is 74 kPa, the energy of each laser is about 120 mJ where the areas of the images in Fig. 5 are all 85 × 45 mm^2. Compared to the experimental results in air, the size of the plasma in combustible gas is smaller than that in air. The glow region around the target should be the area the incomplete combustible wave passed through, as pointed out in the previous experiments [11,17–21]. Using OMA, it was revealed that the radiation of this region mainly comes from the $A^2\sum^+ - X^2\Pi$ band of OH radicals with a wavelength range of 308–320 nm, as shown in Fig. 6. Past experimental results have revealed that the incomplete combustible wave propagates at a surprising speed and that the mechanisms of the production of the glow region remains poorly understood [17–21].

In order to monitor the history of the pressure and ionization at the two points on top of the cell, which are in front of the target and has the same distance to the focal point of the lens, a pressure sensor and an ionization probe are set in place. On one of the sides of the cell, a photodiode with a response wavelength from 0.45 to 1.6 μ is employed for the radiation of the glow region. As shown in Fig. 5(c), the ionization process displays obvious hysteresis to the pressure, and the radiation from 0.45 to 1.6 μ appears 700–800 μs after laser pulse onset as the initial pressure is 74 KPa, under the explosion threshold.

As the pressure of the combustible gas is higher than the threshold of the above explosion, the interaction of laser pulse

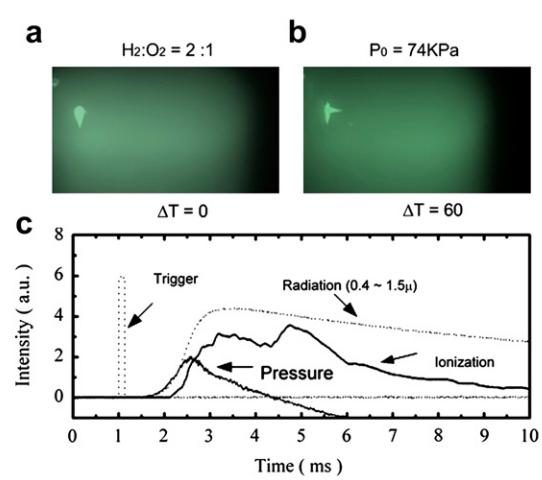

Fig. 5 – Combustion process of the combustible gas with a pressure of 74 kPa and laser energy pulse is about 120 mJ; (a) and (b) the images around the target, and (c) the radiation, pressure, ionization, and trigger signal versus the time.

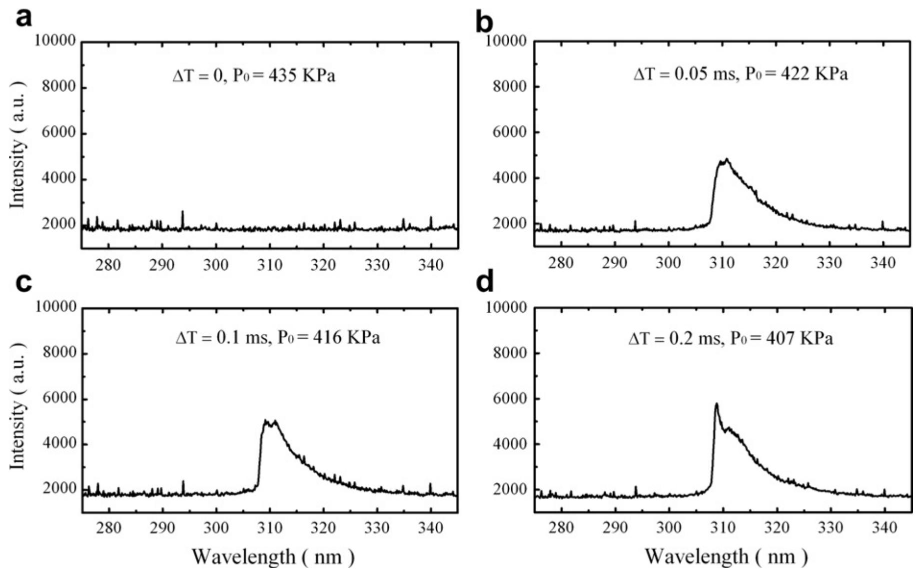

Fig. 6 – Experimental spectra during the incomplete combustion period where the energy of each laser pulse is 300 mJ and the exposure time of OMA is 20 μs with different delay times.

with the target will initiate explosion of the gas. In the ignition period, the images of the ignition point are different from those in the combustion state. Fig. 7(a) and (b) shows the images for $\Delta T = 0$ and $\Delta T = 60$ μs, as the pressure of the gas is 92 kPa and the energy of each pulse is also about 120 mJ. In this experiment, a luminous cone-shaped region, with a diameter of 30 mm and a height of 50 mm, forms in the front of the target 20 μs after the laser pulse onset. From Fig. 7(a), it can be seen that the expansion of this region should gradually develop from the focal point of the lens and the develop in all directions. After a very short time (20–40 μs), the luminous region expands to all the parts of the cell. By comparing the histories of the pressures, the fluctuation of the pressure in the explosion is shown to be much stronger than that in the combustion. This means that the combustion process is more stable than the explosion, as shown in Figs. 5 and 7(c).

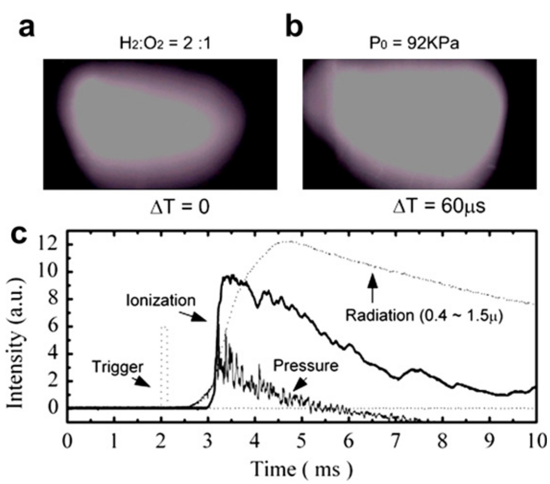

Fig. 7 – Explosion process of the combustible gas with a pressure of 92 kPa as the energy of each laser pulse is about 120 mJ, where (a) and (b) are the images around the target, and (c) the radiation, pressure, ionization, and trigger signal versus the time.

The experimental results also reveal that the radiation of the luminous region still mainly originates from the OH radicals. Moreover, the density of OH radicals in the explosion should be higher than the density in the combustion since the brightness of the images in the explosion is stronger. For the explosion state, the pressure and ionization rise simultaneously and also increase faster than the radiation signal as shown in Fig. 7(c). Before the pressure signal rapidly increased, the slow rising of the pressure signal was attributed to the releasing heat process of the chaining terminal reaction near the ignition point. This process takes place in a low temperature due to the chaining branch reaction where the propagation of the expansion wave is faster than that of the ionization wave. On the other hand, the violent fluctuation of the pressure results from the propagation of the blast waves in all directions and their reflection on the walls of the cell, which is an important feature for the distinction between explosion and combustion.

The minimum ignition energy for the premixed gas of hydrogen and air (H_2:Air = 0.26:1) is estimated experimentally for different pressures. In the ignition process, laser beam provides the energy for not only the ablation of the seed free electron from the heated coal target but also the production of the active radicals through the cascade process for the initiation of the combustion of the gas. The minimum ignition energy is obtained by decreasing the initial pressure of combustible gas and with a fixed laser output. Fig. 8 shows the experimental results on the minimum ignition energy for the ignition of premixed gas of air and hydrogen. It is obvious that the minimum ignition energy is inversely proportional to the initial pressure of the premixed gas, which was also found in the previous experiments on laser ignition by using nanosecond Q-switched lasers by Phuoc [6] and Weinrotter et al.

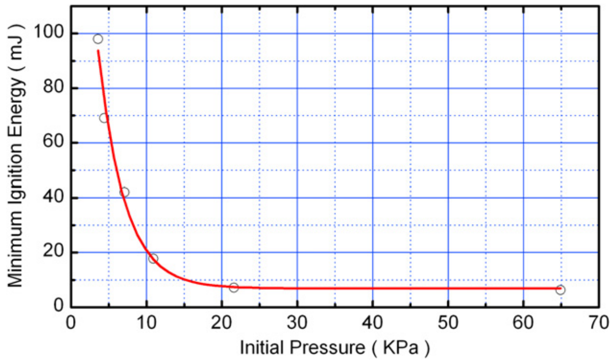

Fig. 8 – Experimental results for the minimum ignition energy at different initial pressures for the combustible gas of hydrogen and air.

[10]. This character is attributed to that the number of the molecules in the focal region is increased and the laser beam can be absorbed more efficiently in the gas with higher initial pressures. As the initial pressure is higher than 20 and 65 KPa, the minimum ignition energies are lower than 7.2 mJ and 6.5 mJ, respectively. Although the different developments of the plasma are found in the air and the combustible gas, as shown in Figs. 3, 4, 5(a) and (b), the free electrons ablated from the target are all indispensable for the initiation of the cascade process and the deposition of the laser energy.

One of the differences of the ignition process via free-oscillated laser pulse from a Q-switched laser pulse is the dimension of the plasma. For a Q-switched laser pulse, the plasma forms immediately through the cascade breakdown effect. For the production of the OH radicals in the combustible gas, however, a much longer period than the duration of a Q-switched laser pulse is required. Therefore, for the laser-induced plasma via Q-switched laser pulse, the tampering or suppressing effect on the plasma due to the existence of the OH radicals is negligible, and plasma can be formed in normal gas or combustible gas. This has been proven by previous experiments on pulsed high-voltage electric discharge and spark induced by a Q-switched laser pulse on a metal target [17,18,21]. For a free-oscillated laser pulse, the active radical is produced in a large amount. As the laser beam interacts with the particle jet from the target and the gaseous molecules, the laser energy is consumed in the chaining branch reaction; therefore, the formation and expansion of the plasma are seriously hindered. Thus, the dimension of the plasma decreases and the light around the target strengthens with the initial pressure under the expansion threshold. However, the mechanism or process of the generation of the glow or luminous region through the interaction of laser beam with gaseous molecules is not yet understood and remains a research issue for the future.

5. Conclusion

In summary, the characteristics of the plasma induced by the interaction between free-oscillated laser pulses with a coal target in the air are experimentally investigated via their images and temperatures. The temperature of the plasma is measured by the fitting of the experimental spectrum structure of $B^2\sum^+ \rightarrow X^2\sum^+$ band of CN radicals with the simulated spectrum. The electron density in the plasma is estimated according to the simplified Kramer formula. A four-frame CCD camera with 20 μs exposure time is employed to capture the plasma images for analysis. The experimental results reveal that the lifetime of the plasma is nearly equal to the duration of the laser pulse since the energy loss of the plasma is compensated by the laser beam. The range of the temperature and the electron density of the plasma are from 5000 K to 9000 K and in the order of 10^{18} cm^{-3}, respectively, as the energy of each laser pulse is in the order of 10^2 mJ. As the interaction above occurs in the premixed combustible gas of hydrogen and oxygen, the formation and development of the plasma are hindered or suppressed by the production of the OH radicals through the chaining branch reaction where the laser pulse provides the energy required in these reactions. This process can initiate the combustion or explosion of the mentioned premixed gas, depending on the initial pressure.

Acknowledgements

The authors acknowledge the financial support from the National Science Foundation of China under Grant No.10472123.

REFERENCES

[1] Shen YR. The principle of nonlinear optics. New York: John Wiley & Sons; 1984. Chapter 27, pp. 528–530.
[2] Lavid M, Stevens JG. Photochemical ignition of premixed hydrogen/oxidizer mixtures with excimer lasers. Combustion and Flame 1985;60:195–202.
[3] Bonald Lucas, Derek Dunn-Rankin, Kenneth Hom, Brown Nancy J. Ignition by excimer laser photolysis of ozone. Combustion and Flame 1987;69:171–84.
[4] Smith David C. Gas-breakdown dependence on beam size and pulse duration with 10.6 μwavelength radiation. Applied Physics Letters 1971;19(10):405–8.
[5] Ramsden SA, Davies WER. Radiation scattered from the plasma produced by a focused ruby laser beam. Physical Review Letters 1964;13(7):227–9.
[6] Phuoc Tran X. Laser-induced spark ignition fundamental and application. Optics and Laser in Engineering 2006;44: 351–97.
[7] JianMa X, Alexander Dennis R, Poulain Dana E. Laser spark ignition and combustion characteristics of methane-air mixture. Combustion and Flame 1998;112:492–506.
[8] Zhang Hongchao, Lu Jian, Shen Zhonghua, Ni Xiaowu. Investigation of 1.06 μm laser induced plasma in air using optical interferometry. Optics Communications 2009;282: 1720–3.
[9] Srivastava DK, Weinrotter M, Iskra K, Agarwal AK, Wintner E. Characterisation of laser ignition in hydrogen-air mixtures in a combustion bomb. International Journal of Hydrogen Energy 2009;34:2475–82.
[10] Weinrotter M, Kopecek H, Wintner E, Lackner M. Application of laser ignition to hydrogen–air mixtures at high pressures. International Journal of Hydrogen Energy 2005;30:319–26.

[11] Kossyi IA, Silakov VP, Tarasova NM, Wie D van. Long-lived plasmoids generated by surface laser sparks in combustible gas mixtures. Plasma Physics Reports 2006;32(4):349–51.
[12] Brown Robert T, Smith David C. Laser-induced gas breakdown in the presence of preionization. Applied Physics Letters 1973;22(5):245–7.
[13] Gill Dennis H, Dougal Arwin A. Breakdown minima due to electron-impact ionization in super-high-pressure gases irradiated by a focused giant-pulse laser. Physical Review Letters 1965;15(22):845–7.
[14] Ram RS, Davis SP, Wallace L, Engleman R, Appadoo DRT, Bernath PF. Fourier transform emission spectroscopy of $B^2\sum^+ \rightarrow X^2\sum^+$ system of CN. Journal of Molecular Spectroscopy 2006;237:225–31.
[15] Melendez FJ, Sandoval L, Palma A. Franck–Condon factors for diatomic molecules with anharmonic corrections. Journal of Molecular Structure (Theochem) 2002;580:91–9.
[16] Yang Qiansuo, Liu Chun, Peng Zhimin, Zhu Naiyi. Laser-induced particle jet and its ignition application in premixed combustible gases. Chinese Physics Letters 2009;26(6):065204.
[17] Kazantsev SYu, Kononov IG, Kossyi IA, Tarasova NM, Firsov KN. Ignition of a combustible gas mixture by a laser spark excited in the reactor volume. Plasma Physics Reports 2009;35:251–7.
[18] Grytsinin SI, Kossyi IA, Misakyan MA, Silakov VP, Tarasova NM, Temchin SM. Features of gaseous mixtures combustion initiated by high-current slipping surface discharge. Journal of Thermophysics and Heat Transfer 2002; 16(3):450–4.
[19] Kossyi IA, Silakov VP, Tarasova NM, Taktakishvili MI, Wie D van. Long-lived plasmoids as initiators of combustion of gas mixture. Plasma Physics Reports 2004;30(4):375–84.
[20] Berezhetskaya NK, Gritsinin SI, Kop'ev VA, Kossyi IA, Wie D van. Long-lived plasmoids generated by surface microwave discharges in chemically active gases. Plasma Physics Reports 2005;31(10):886–90.
[21] Berezhetskaya NK, Gritsinin SI, Kop'ev VA, Kossyi IA, Kuleshov PS, Popov NA, et al. Ignition of combustible gas mixture by a high-current electric discharge in a closed volume. Plasma Physics Reports 2009;35(6):471–83.